# ADYTrack: Development of a Railroad Trackbed Model and Parametric Study of Track Modulus

A. Arshid[1], Y. Huang[2] and D. Tolliver[3]
[1,2]*Department of Civil and Environmental Engineering, North Dakota State University, Fargo-ND, USA*
[3]*Upper Great Plains Transportation Institute, North Dakota State University, Fargo-ND, USA*
*E-mail*: ying.huang@ndsu.edu

**ABSTRACT:** Deformation prediction of railroad trackbed has always been a challenge for the railroad designers and engineers. There are many complex interactions take place simultaneously between superstructure and subgrade of railways trackbed, which simply make the deformation predictions harder. Numerical models offer an alternative to simulate the performance of the substructure of railroad with considerable accuracy. In this paper, a finite element based three-dimensional (3D) model has been developed in MATLAB. This model has the capability to study the effects of track modulus, subgrade modulus, interactions between track and soil, the track geometry, and the wheel loads. The rails and ties are modelled as two node beam (line) elements and the substructure (ballast, subgrade etc.) is modelled as eight node isoperimetric hexahedron brick elements. The rail-tie interaction is modelled using a liner elastic spring elements. The model was first calibrated against an identical model built ANSYS (APDL), a reliable commercial software. The results of the ADYTrack are further validated with other numerical models and full-scale field test results reported in the literature. Following successful validation, a detailed parametric study is conducted to study the response of track modulus for a typical All-Granular trackbed using practical range of values for the variables involved. Numerical analysis showed that subgrade resilient modulus substantially impacts the track modulus. Furthermore, the depth of the ballast, moment of inertia of rail beams and tie spacing reasonably affected the track modulus, in a decreasing order.

**KEYWORDS:** Railroad, Numerical Models, Finite Element Analysis, Subgrade Soil, Track Modulus

## 1. INTRODUCTION

Railroad trackbed analysis and design has always been a challenge due to many reasons. For instance, different materials involved (Steel, wood, concrete, soils), complex interactions at the interfaces of those materials, and variations in granular especially subgrade soils, are just to name a few. Practitioners have been heavily relying on field testing and empirical solutions in the past, with primary focus on safety. As the advent of computing technologies and introduction of analytical models, the idea of optimal design proliferated.

Many researchers have proposed different models to predict the stresses and strains (or displacements) in different components of the railroad trackbed structure. The Beam on Elastic Foundation (BOEF) theory provided the earliest theoretical solution framework [Clarke (1957), Hetenyi (1946), Meacham et. al. (1968), Selvadurai (1979), Talbot (1933)] for analysis and design of pavements. Winkler (1865) used the Euler-Bernoulli beam supported by elastic foundation. He assumed the reaction forces are function of beam deflection at any given point along the beam under the application of externally applied loads. Burmister then introduced multilayer elastic theory [Burmister (1945)], which facilitated many researchers to model the substructure with different materials.

The BOEF theory upgraded by incorporating the multilayer elastic theory [Burmister (1945)], brought the earliest railroad numerical models including MULTA [Selig et al. (1979)]. MULTA model used Burmister's multilayers elastic theory in conjunction with structural analysis models to solve a three-dimensional model for tie-ballast reactions [Adegoke et. al. (1979)]. Some of its limitations included the inability to allow relative displacement between tie and ballast and all forces were in vertical direction only ignoring shear forces.

Another breakthrough was the introduction of Finite Element (FE) methods [Bathe and Wilson (1976), Pichumani (1973), Strang and Fix (1973), Zienkiewicz and Cheung (1965), Zienkiewicz (1977)] and its applications for pavement designs. Chang et. al. built a model, named PSA, on the fundamentals of FE methods with prismatic element types for substructure [Chang (1975), Chu et. al. (1977), Crawford (1972), Herrmann (1968)]. It also separated the substructure from superstructure for the response calculations while maintaining the continuity conditions, baseline of FE analysis. This offered some advantage over MULTA including allowing to change the material properties along the tie and across the rail beam and computational economical when compared with models using brick elements.

ILLITRACK [Robnett et. al. (1976), Tayabji and Thompson (1976a), Tayabji and Thompson (1976b)] combined the two-dimensional analysis and longitudinal direction followed by traverse direction two-dimensional analysis, thus formulating a quasi-three-dimensional finite element analysis. The model attempted to model the non-linearity and stress dependant response of materials to simulate the physical problem more accurately. The resilient modulus ($E_r$), a ratio of cyclic stress to the corresponding recoverable strain, as given by Equation (1) was used to model the nonlinearity of ballast and subballast [Monismith and Finn (1975), Barksdale 1975]:

$$E_r = K_1 \theta^{K2}, \tag{1}$$

where $K_1$ and $K_2$ are soil parameters obtained from the laboratory testing. The major drawback of the model was its pseudo-three-dimensional assumption.

Later, GEOTRACK was proposed by Chang et al. (1980), which was a multilayer theory based three-dimensional model which was recently upgraded GEOTRACK for railroad track analysis [Mishra et. al. (2016)] with Graphical User Interface (GUI) features. GEOTRACK was built on the fundamentals of multilayer theory with quasi-dynamic loading conditions [Chang el. al. (1980), Mishra et. al. (2016), Stewart and Selig (1982), Stewart (1988)]. It also considered the nonlinear and stress dependent behaviour of materials and kept ties separated from the substructure. The model's primary focus was on the geotechnical response of the trackbed. The model considered eleven ties with wheel load applied at the mid-tie, assuming complete distribution of applied stresses by the fifth tie [Selig and Waters (1994)]. Rail and ties are modelled as linear elastic beams, whereas substructure was modelled as linear elastic layers. This model was developed based on PSA and MULTA code while introducing some improvements.

Huang et al. introduced KENTRACK based on same multilayer theory and FEA to calculate stresses and strains in substructure. KENTRACK is finite element based multi-layered elastic model developed in the University of Kentucky [Huang et. al. (1984), KENTRACK (2006), Li et. al. (2015), Liu (2013), Rose et. al. (2000) (2010) (2014)]. The model was capable of prediction not only the response of the trackbed but also the cumulative damage caused by the cyclic loadings of the train operations. This model is also capable of analysing three different types of trackbeds: a) all granular layers trackbed (typical); b) asphalt layered trackbed (replacing subballast with asphalt) and c) combined (subballast plus asphalt) layered trackbed. The failure criteria for the design procedure is cumulative vertical stresses at the top of subgrade or tensile stain at the bottom of asphalt layer, whichever occurs first. The material properties are considered as stress dependent nonlinear as presented by Equation (1). The bottom most layer is assumed to be incompressible to simulate the bedrock conditions.

3D20N is another three-dimensional linear elastic FEA based model [Shahu et al. (1999)]. This model also considered the full geometry of the railways track. This model used 20-noded isoparametric hexahedral (aka brick) elements for substructure layered materials, whereas rail and ties are modelled as 1-D beam elements. All the interfaces are modelled as zero thickness 16-noded surface elements to allow relative movement between different materials and surfaces. The model uses only one fourth of the model due symmetric loading conditions and geometry and spans over five ties only. The boundary conditions are set such that the surfaces along axis of symmetries and the bottom most surface were constraint for normal movements while allowing movement in other two directions.

Feng Huang (2011) compared several models for their advantages, disadvantages and their predictions. Of all these models, GEOTRACK and KENTRACK are the most common among researchers and practitioners. Both these programs have their merits and demerits. However, some of their limitations as studied by Feng Huang (2011) are as under:

1) It is likely to miss the maximum stresses due the fact that loads are applied directly above the supports, while using GEOTRACK;
2) GEOTRACK assumes rail as a beam of finite length, and do not consider the jointing effects;
3) Neither of these models account for time dependant response of materials;
4) None of these models consider dynamic effects of rail operations;
5) Use of linear elastic models to similar soil behaviour can cause considerable errors;
6) The effects of lateral forces are neglected altogether.

The objective of this study is to develop a numerical model to address these limitations listed above, named ADYTrack. A detailed description of the model is presented in the following section explaining the model geometry, loading and boundary conditions, mechanics of 8-nodal isoperimetric hexahedral brick elements. Then, the predictions of the model are validated against the other well-known models.

## 2. ADYTRACK MODEL

ADYTrack is a finite element based three-dimensional (3-D) model, built in MATLAB programming language, which can analyse the railroad trackbed, ideally for infinite number of layers. The model provides the use with a lot of liberty in choosing the number of ties to consider, number of layers to constitute substructure, rail type, gauge length, tie type, tie spacing, wheel load application location and so on. The model is built with full geometry without taking advantage of axis symmetries to accommodate future extensions. The cross section of the trackbed with all its components is shown in Figure 1.

The model is fundamentally based on finite element analysis, the details of which can be found in the literature [Chandrupatla and Belegundu (1997)]. The rails and ties are modelled as 2-nodal beam elements with full six degrees of freedom ($u_x$, $u_y$, $u_z$, $\sigma_x$, $\sigma_y$, $\sigma_z$) at each node. The rail elements transmit the load to ties through a 1-D spring element, capable of withstanding tensions and compressions. The current version of the model considers only one axle (two wheel) loading and applies at the nodes corresponds to the user defined tie number.

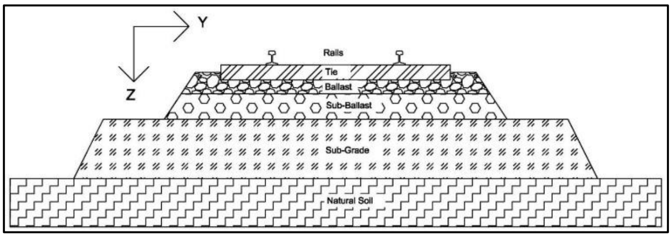


Figure 1 Cross section of the trackbed

All the granular layers (ballast, subballast, subgrade and natural soil) are modelled as 8-nodal isoperimetric hexahedral brick elements. One can define as many main layers (ballast, sub-ballast etc.) as he needs to and can further uniformly divide each main layer into any number of sublayers. The thickness of each sublayer is considered as the thickness of brick elements in that corresponding sublayer. Material properties of these layers, which include Young's modulus of elasticity and Poison's ratio, are assumed as linear elastic in this first version of the model. Gravitational weights of these brick elements, defined by their unit weights are considered as body forces in the analysis. Instead of assuming homogeneous half space for all these layers, a more realistic geometry is considered including shoulder width at the top and side slope for each main layer (Figure 1). Corner nodes of these brick elements are numbered systematically to minimize the efforts to construct node-element connectivity table which is shown in Figure 2.

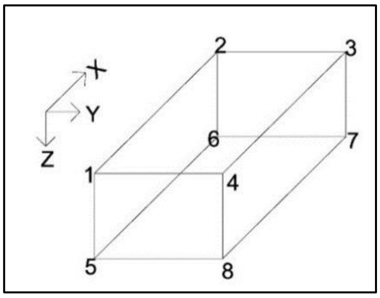


Figure 2 Brick element node (corner) numbering

Boundary conditions applied to the nodes constituting rail and tie elements allow all movements except buckling and torsion. This simulates the absence of fasteners, which will not affect the results as the loading conditions are static and vertical. To ensure the global stability of the model, movements are constraint in three different planes. Vertical movement ($u_z$=0) is constraint for the bottom most layer of nodes. Longitudinal movement ($u_x$=0) is restricted at x=0, i.e., at the first tie location in YZ-plane. And lastly, the tangential movement ($u_y$=0) is constrained at y=0, i.e., along the middle of both rail in XZ-plane. The element stiffness matrix for beam elements is presented in Equation (2) in local coordinates system.

$$\mathbf{K'} = \begin{bmatrix} AS & 0 & 0 & 0 & 0 & 0 & -AS & 0 & 0 & 0 & 0 & 0 \\ & a_z' & 0 & 0 & 0 & b_z' & 0 & -a_z' & 0 & 0 & 0 & b_z' \\ & & a_y' & 0 & -b_y' & 0 & 0 & 0 & -a_y' & 0 & -b_y' & 0 \\ & & & TS & 0 & 0 & 0 & 0 & 0 & -TS & 0 & 0 \\ & & & & c_y' & 0 & 0 & 0 & b_y' & 0 & d_y' & 0 \\ & & & & & c_z' & 0 & -b_z' & 0 & 0 & 0 & d_z' \\ & & & & & & AS & 0 & 0 & 0 & 0 & 0 \\ & & & & & & & a_z' & 0 & 0 & 0 & -b_z' \\ & & & & & & & & c_y' & 0 & b_y' & 0 \\ & & & & & & & & & TS & 0 & 0 \\ & & & & & & & & & & c_y' & 0 \\ S & y & m & m & e & t & r & i & c & & & c_z' \end{bmatrix} \tag{2}$$

where AS=EA/$l_e$, $l_e$=length of the element, TS=GJ/$l_e$, $a_z$'=12E$I_z$'/$l_e^3$, $b_z$'=6E$I_z$'/$l_e^2$, $c_z$'=4E$I_z$'/$l_e$, $d_z$'=2E$I_z$'/$l_e$, $a_y$'=12E$I_y$'/$l_e^3$, and so on. In these expressions, E, A, G, J, $I_y$', $I_z$' are Young's elastic modulus, cross sectional area, shear modulus, polar moment of inertia, second moment of area along y- and z-axis respectively. The element stiffness matrix in global coordinates system can be found using Equation (3),

$$K = L^T K' L, \tag{3}$$

where

$$\mathbf{L} = \begin{bmatrix} \boldsymbol{\lambda} & \mathbf{0} & \mathbf{0} & \mathbf{0} \\ & \boldsymbol{\lambda} & \mathbf{0} & \mathbf{0} \\ & & \boldsymbol{\lambda} & \mathbf{0} \\ & & & \boldsymbol{\lambda} \end{bmatrix} \qquad \boldsymbol{\lambda} = \begin{bmatrix} l_1 & m_1 & n_1 \\ l_2 & m_2 & n_2 \\ l_3 & m_3 & n_3 \end{bmatrix}$$

in which, $l_1 = \dfrac{x_2 - x_1}{l_e}$ , $m_1 = \dfrac{y_2 - y_1}{l_e}$ , and $n_1 = \dfrac{z_2 - z_1}{l_e}$ .

The element stiffness matrix for brick elements is calculated using Equation (4) as below:

$$\mathbf{K}^{(e)} = \sum_{i=1}^{p_1} \sum_{j=1}^{p_2} \sum_{k=1}^{p_3} \omega_{ijk} \mathbf{B}_{ijk}^{\mathbf{T}} \mathbf{E} \mathbf{B}_{ijk} J_{ijk} \tag{4}$$

where, $p_1$, $p_2$ and $p_3$ denote the number of Gauss points (using a product rule of integration and same number of points in every direction, i.e., 2) in the neutral axis directions respectively, whereas $w_{ijk}$, $B_{ijk}$, E and $J_{ijk}$ are weight of Gauss integration, Strain-Displacement matrix, Stress-Strain matrix and determinant of Jacobian matrix respectively.

Equation (5) present the strain-displacement relationship which is used to calculate element strains after the whole system is solved for nodal displacements. The B matrix is calculated by taking partial derivatives of shape function with respect to global coordinates (x, y, and z). These partial derivatives are calculated using Equation (6).

$$\mathbf{B} = \begin{bmatrix} \frac{\partial N_1^e}{\partial x} & 0 & 0 & \frac{\partial N_2^e}{\partial x} & 0 & 0 & \cdots & \frac{\partial N_8^e}{\partial x} & 0 & 0 \\ 0 & \frac{\partial N_1^e}{\partial y} & 0 & 0 & \frac{\partial N_2^e}{\partial y} & 0 & \cdots & 0 & \frac{\partial N_8^e}{\partial y} & 0 \\ 0 & 0 & \frac{\partial N_1^e}{\partial z} & 0 & 0 & \frac{\partial N_2^e}{\partial z} & \cdots & 0 & 0 & \frac{\partial N_8^e}{\partial z} \\ \frac{\partial N_1^e}{\partial y} & \frac{\partial N_1^e}{\partial x} & 0 & \frac{\partial N_2^e}{\partial y} & \frac{\partial N_2^e}{\partial x} & 0 & \cdots & \frac{\partial N_8^e}{\partial y} & \frac{\partial N_8^e}{\partial x} & 0 \\ 0 & \frac{\partial N_1^e}{\partial z} & \frac{\partial N_1^e}{\partial y} & 0 & \frac{\partial N_2^e}{\partial z} & \frac{\partial N_2^e}{\partial y} & \cdots & 0 & \frac{\partial N_8^e}{\partial z} & \frac{\partial N_8^e}{\partial y} \\ \frac{\partial N_1^e}{\partial z} & 0 & \frac{\partial N_1^e}{\partial x} & \frac{\partial N_2^e}{\partial z} & 0 & \frac{\partial N_2^e}{\partial x} & \cdots & \frac{\partial N_8^e}{\partial z} & 0 & \frac{\partial N_8^e}{\partial x} \end{bmatrix} \tag{5}$$

$$\begin{bmatrix} \frac{\partial N_i^e}{\partial x} \\ \frac{\partial N_i^e}{\partial x} \\ \frac{\partial N_i^e}{\partial x} \end{bmatrix} = \begin{bmatrix} \frac{\partial \xi}{\partial x} & \frac{\partial \eta}{\partial x} & \frac{\partial \mu}{\partial x} \\ \frac{\partial \xi}{\partial y} & \frac{\partial \eta}{\partial y} & \frac{\partial \mu}{\partial y} \\ \frac{\partial \xi}{\partial z} & \frac{\partial \eta}{\partial z} & \frac{\partial \mu}{\partial z} \end{bmatrix} \begin{bmatrix} \frac{\partial N_i^e}{\partial \xi} \\ \frac{\partial N_i^e}{\partial \eta} \\ \frac{\partial N_i^e}{\partial \mu} \end{bmatrix} = \mathbf{J}^{-1} \begin{bmatrix} \frac{\partial N_i^e}{\partial \xi} \\ \frac{\partial N_i^e}{\partial \eta} \\ \frac{\partial N_i^e}{\partial \mu} \end{bmatrix} \tag{6}$$

Jacobian matrix (J), presented in Equation (6) is a product of nodal values presented in Equation (7) and partial derivatives of shape function w.r.t. to natural axis ( $\xi$ , $\eta$ , $\mu$ ).

$$\mathbf{J} = \begin{bmatrix} x_i \frac{\partial N_i^e}{\partial \xi} & y_i \frac{\partial N_i^e}{\partial \xi} & z_i \frac{\partial N_i^e}{\partial \xi} \\ x_i \frac{\partial N_i^e}{\partial \eta} & y_i \frac{\partial N_i^e}{\partial \eta} & z_i \frac{\partial N_i^e}{\partial \eta} \\ x_i \frac{\partial N_i^e}{\partial \mu} & y_i \frac{\partial N_i^e}{\partial \mu} & z_i \frac{\partial N_i^e}{\partial \mu} \end{bmatrix} \tag{7}$$

$$\begin{bmatrix} 1 \\ x \\ y \\ z \end{bmatrix} = \begin{bmatrix} 1 & 1 & 1 & 1 & 1 & 1 & 1 & 1 \\ x_1 & x_2 & x_3 & x_4 & x_5 & x_6 & x_7 & x_8 \\ y_1 & y_2 & y_3 & y_4 & y_5 & y_6 & y_7 & y_8 \\ z_1 & z_2 & z_3 & z_4 & z_5 & z_6 & z_7 & z_8 \end{bmatrix} \begin{bmatrix} N_1^e \\ N_2^e \\ \cdots \\ N_8^e \end{bmatrix} \tag{8}$$

The shape function (N) of brick elements in its indicial form is presented in Equation (9), whereas values of i[th] node (corner) of the elements are presented in Table 1.

$$N_i^e = \frac{1}{8}(1 + \xi\xi_i)(1 + \eta\eta_i)(1 + \mu\mu_i) \tag{9}$$

Table 1 Natural coordinates at the corners of brick elements

| Node | $\xi$ | $\eta$ | $\mu$ | Node | $\xi$ | $\eta$ | $\mu$ |
|---|---|---|---|---|---|---|---|
| 1 | -1 | -1 | -1 | 2 | +1 | -1 | -1 |
| 3 | +1 | +1 | -1 | 4 | -1 | +1 | -1 |
| 5 | -1 | -1 | +1 | 6 | +1 | -1 | +1 |
| 7 | +1 | +1 | +1 | 8 | -1 | +1 | +1 |

The stress-strain matrix (E) is a symmetric material matrix which remains constant for each element and can be calculated using Equation (10).

$$\mathbf{E} = \frac{E_c}{(1+\upsilon)(1-2\upsilon)} \begin{bmatrix} 1-\upsilon & \upsilon & \upsilon & 0 & 0 & 0 \\ \upsilon & 1-\upsilon & \upsilon & 0 & 0 & 0 \\ \upsilon & \upsilon & 1-\upsilon & 0 & 0 & 0 \\ 0 & 0 & 0 & 0.5-\upsilon & 0 & 0 \\ 0 & 0 & 0 & 0 & 0.5-\upsilon & 0 \\ 0 & 0 & 0 & 0 & 0 & 0.5-\upsilon \end{bmatrix} \tag{10}$$

where, $E_c$ is Young's modulus (or Elastic modulus) and v is Poison's ratio. Finally, the global stiffness matrix is constructed, which will be used for solving nodal displacements using the equation, *F=Kd*.

Nodes of the trackbed considered by ADYTrack for analysis are presented in Figure 3. Solid red lines and blue dots are representing the rails and nodes of the trackbed system respectively. This figure also illustrates the mesh size of the system, as these nodes are used to generate both line and brick elements.

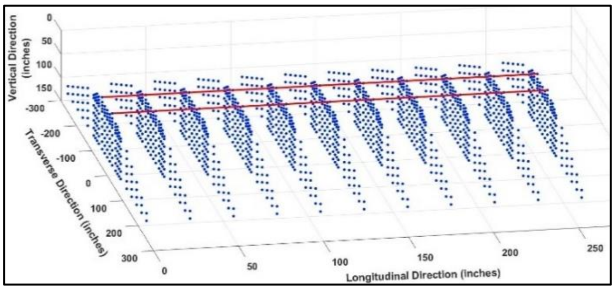


Figure 3 Nodal skeleton of full size trackbed model built in the ADYTrack

## 3. MODEL VALIDATION

To validate any newly developed model, it must pass some standard set of problems. Many researchers have proposed some standard problems [Chen and Cheung (1992), Jog (2005), MacNeal and Harder (1985), Sze and Fan (1996)]. Among those standard tests, straight cantilever beam model is considered quite reliable among the researchers' due to its simplicity and versatility. By varying the loading directions and elements shapes, different deformation modes can be examined. Therefore, the authors also selected the same model to test the ADYTrack using three different elements shapes including rectangular, trapezoidal and parallelogram, as shown in Figure 4. The length, width (our-of-plane) and depth (in-plane) of the beam are 6.0, 0.2 and 0.1 respectively. The material properties are selected as modulus of elasticity equals 1.0×107 and poisons ratio equals 0.30 with standard mesh of 6×1 [MacNeal and Harder (1985)]. The beam is tested for three types of loadings, namely extension, in-plane shear and out-of-plane shear, applied at the tip of the beam. The theoretical tip deformations due to extension, in-plane shear and out-of-plane shear forces are 3.0×10-5, 0.1084 and 0.4321 respectively.

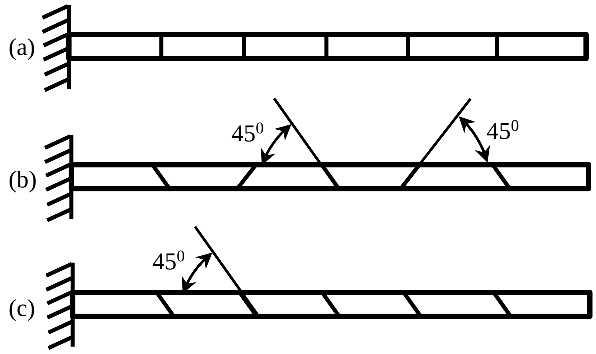


Figure 4 Geometry and element shapes of benchmark cantilever beam model [41]. (a) Rectangular brick elements, (b) Trapezoidal brick elements and (c) Parallelogram brick elements

Table 2 summarizes the normalized tip displacements calculated by ADYTrack using hexahedral 8-noded brick elements, MSC/NASTRAN using HEXA (8) element [MacNeal and Harder (1985)] and ANSYS (APDL) using Solid185 element type. The results show that ADYTrack model captured the response with more than 99% accuracy with all three types of elements against axial loadings. Also, both ADYTrack and HEXA unreliably predicted (with less than 20%) the tip deformations against shear loadings using non-rectangular element shapes with the standard mesh. However, ADYTrack and APDL heavily underpredicted the response with rectangular element and non-extension loading conditions, i.e., 41.2% and 2.6% for in-plane shear and 10.3% and 10% for out-of-plane shear respectively. This underprediction substantially jumped to more than 75% by slightly refining the mesh of ADYTrack model, for both cases of shear loadings.

Aspect ratio of brick element sometimes plays a major role in the prediction of deformation and stress analysis. Therefore, the authors also examined the effect of aspect ratio on the tip deformation calculations for both ADYTrack and APDL models using rectangular elements shapes and out-of-plane shear force and the results are presented in Figure 5. It is evident from the figure that the deformation predicted by APDL element is inversely proportional to its prediction and gives best results in the range of 1:4 aspect ratio. On the other hand, ADYTrack element is found independent of aspect ratio and it can accurately predict the response with aspect ratio as high as 40. In the same study, it is observed that meshing along the bending and along the loading direction plays major and minor roles respectively, whereas traverse direction meshing almost do not affect the results at all.

Table 2 Normalized Tip Displacement in the Direction of the Load

| | ADYTrack | | HEXA (8) | APDL |
|---|---|---|---|---|
| | Rectangular | | | |
| Extension | 0.993 | 0.993 | 0.988 | 0.995 |
| In-Plane Shear | 0.760* | 0.412 | 0.981 | 0.026 |
| Out-of-Plane Shear | 0.798** | 0.103 | 0.981 | 0.100 |
| | Trapezoidal | | | |
| Extension | 0.998 | 0.998 | 0.989 | |
| In-Plane Shear | 0.135* | 0.093 | 0.069 | |
| Out-of-Plane Shear | 0.048** | 0.014 | 0.051 | |
| | Parallelogram | | | |
| Extension | 0.998 | 0.998 | 0.989 | |
| In-Plane Shear | 0.369* | 0.206 | 0.080 | |
| Out-of-Plane Shear | 0.164** | 0.025 | 0.055 | |

*meshing size (7 x 1 x 1)
**meshing size (10 x 1 x 1)

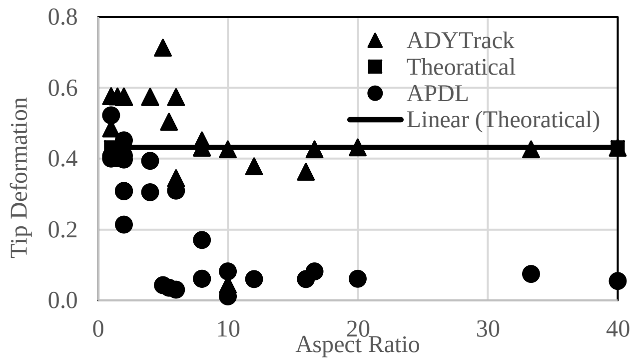


Figure 5 Effect of aspect ratio on the tip displacement of cantilever beam model using APDL and ADYTrack

Figure 6(a) shows the vertical displacement of the model built in the APDL software. The maximum displacement of 1.9 mm is observed below the wheel load and it reduces when moving away along the rail and moving down along the depth. Also, the firth tie experienced almost zero displacement, thus confirming the assumption that the load will be completely distributed by the fifth tie. The vertical stress distribution at the cross sections cut below at each tie is shown in Figure 6(b). The stress distribution is following a typical trend, highest below the wheel load and faded away as the distance increases from wheel load long the rail and along the depth. The stresses observed at the top of ballast, subballast and subgrade by APDL model are as 550 kPa, 110 kPa and 55 kPa respectively. Using symmetries, a section of trackbed spanning five ties and half of wheel load is considered for this study as Feng Huang (2011) noted that applied load influences a zone of approximately five ties on each side. Most of the parameters required to build the model were available, however, the depth of subgrade could not be found for all these models. A subgrade depth of 2.0 m is used for the ADYTrack model. The subgrade depth is found to be a considerable contributor to the total displacement of the trackbed in ADYTrack model.

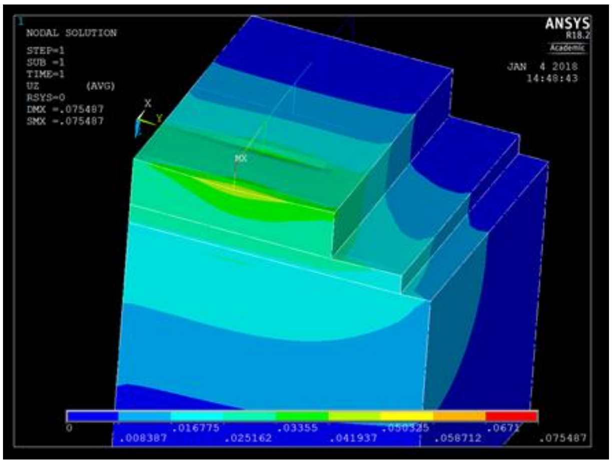


Figure 6(a) Vertical displacement (inches) contour plot of the trackbed model in the APDL model

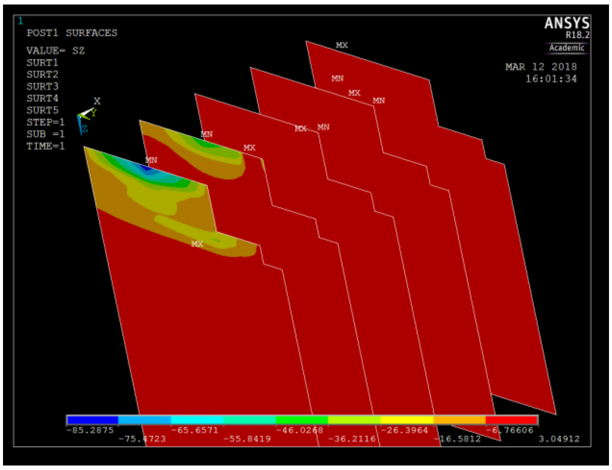


Figure 6(b) Vertical stress (psi) contour plot of the trackbed model in the APDL model.

The trackbed displacement calculated by ADYTrack model are validated through comparisons with analysis results from other models, including the 3D20N model and the MULTA model (base model for GEOTRACK), PSA and ILLITRACK. The important properties of the trackbed geometry and the materials are summarized in Table 3. Figure 7(a) compares the vertical displacements along the depth of the trackbed below wheel load using different models including ADYTrack. Selig at al. (1979) and Shahu et al. (1999) predicted the response of the trackbed for the field tests conducted at the facilities of FAST research centre using their models, MULTA (GEOTRACK), PSA, ILLITRACK and 3D20N respectively. It is evident in the figure that the largest displacements predicted by all the models is at the top of the ballast and it gradually reduces as the depth increases. It is also evident in the figure that the ADYTrack model predicted the trackbed deformations quite reasonably. The ADYTrack predictions for vertical displacement along the depth are closer to PSA (GEOTRACK), MULTA and 3D20N model predictions with an overall difference of about 10 %. Only the ILLITRACK predictions are significantly (more than 100%) deviating from the rest of the predictions.

The variation in vertical stresses with depth below the wheel load are plotted in Figure 7(b). It is evident in the figure that ADYTrack captured the overall stress distribution along the depth of trackbed with reasonable accuracy. The predicted stresses by the ADYTrack are again close to PSA with negligible difference (less than 5% deviation). However, it overestimated the stresses by almost 75 % at the top of subgrade when compared with MULTA and 3D20N model predictions, whereas it underestimated the vertical stresses at the top of subgrade when compared with ILLITRACK by around 36%.

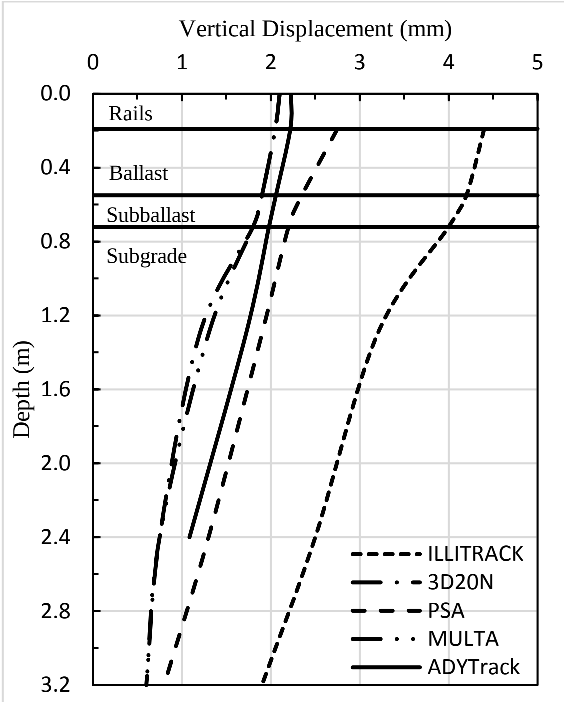


(a)

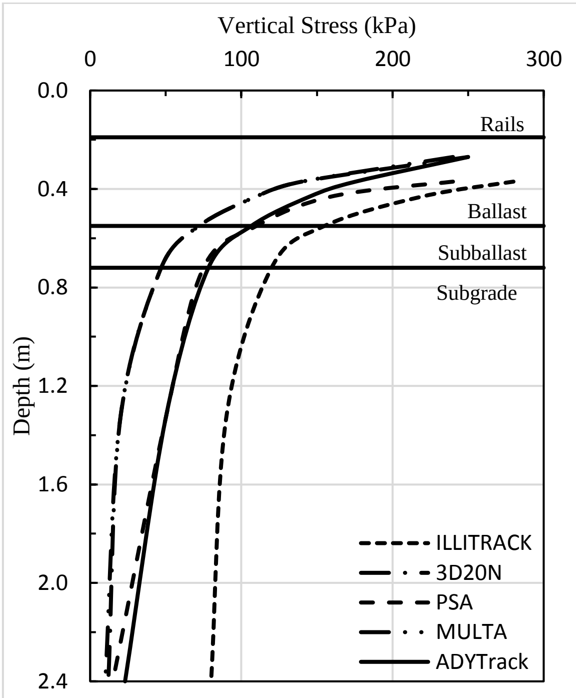


(b)

Figure 7 (a) Vertical displacement and (b) vertical stress along the depth below the wheel load using different models.

## 4. PARAMETRIC STUDY

A detailed parametric study is conducted for a virtual railways trackbed with its important properties summarized in Table 3. The track responses selected for this study were rail and tie displacements, vertical stresses at the top of ballast, subballast and subgrade right below the wheel load, applied the first tie.

Table 3 Constant Track Properties for Parametric Study

| Properties | Nominal Value |
|---|---|
| Rail | |
| Rail Section | RE110 |
| Modulus, Er | 207,000 MPa |
| Poison's Ratio | 0.30 |
| Guauge Length | 1435 mm |
| Tie | |
| Modulus, Er | 10,340 MPa |
| Poison's Ratio | 0.37 |
| Spacing | 550 mm |
| Length | 2500 mm |
| Width | 225 mm |
| Thickness | 175 mm |
| Ballast | |
| Depth | 350 mm |
| Modulus, Es | 207 |
| Poison's Ratio | 0.37 |
| Subballast | |
| Depth | 150 mm |
| Modulus, Esb | 138 |
| Poison's Ratio | 0.37 |
| Subgrade | |
| Depth | 2000 mm |
| Modulus, Esg | 35 |
| Poison's Ratio | 0.33 |
| Rail-Tie Spring Constant | 1,225 kN/mm |
| Wheel Load | 160 kN |

The track responses were studied against the variations in modulus and depths of substructure granular layers, the summery of which is presented in Table 4. The track responses are calculated at the nodes right below the wheel load and belong to left hand side of the rail track (between centerline and rail beam).

Table 4 Track Properties used for Parametric Study

| Properties | Nominal Value | Variations in values |
|---|---|---|
| Modulus (MPa) | | |
| Ballast (Eb) | 207 | 150, 250 |
| Subballast (Esb) | 138 | 100, 200 |
| Subgrade (Esg) | 35 | 10, 60 |
| Depth of Layer (mm) | | |
| Ballast (Db) | 350 | 250, 750 |
| Subballast (Dsb) | 150 | 100, 450 |
| Subgrade (Dsg) | 2000 | 1500, 3000 |
| Rail Moment of Inertia (Ir) ($cm^4$) | 2040 | 1500, 3000 |

The track responses (dependent variables) and changing variables (independent variables) are presented in Figure 8 to 10 and are compared against the nominal values for the same response variable. The response of trackbed in terms of rail and tie displacements are plotted in Figures 8 (a, b). It is evident that the modulus of subgrade has the most impact on both the rail and the tie displacements, followed by depth of subgrade. Rest of the varying parameters do not affect rail and tie displacements significantly, as noted by Shahu et. al. (1999) as well. A reduction in subgrade modulus from 60 MPa to 10 MPa can increase the rail and tie vertical deformations by 4.5 times. On the other hand, reduction in depth of subgrade from 3000 mm to 1500 mm can double the rail and tie vertical deformations under the wheel load.

The vertical stress at the top of ballast surface is most affected by the depth of ballast and modulus of subgrade, as shown in Figure 9(a). By increasing the depth of ballast from 250 mm to 750 mm can cause about 40% reduction in the stress. Similarly, increase in subgrade modulus from 10 MPa to 60 MPa can reduce the stresses up to 30%. The modulus of ballast and depth of subballast can reduce the stress between 15% and 20% when varied from 150 MPa to 250 MPa and 1500 mm to 3000 mm respectively. Rail moment of inertia has slight affect in the reduction of the stress (up to 5%).

Figure 9(b) shows that the depth of ballast has the most potential to affect the vertical stress at the top of subballast layer. A reduction in which from 750 mm to 250 mm can increase the stresses in the subballast by 500%. The second most affecting variable is subgrade modulus, which can cause an increase of almost 100% when decreased from 60 MPa to 10 MPa. Depth of subgrade and modulus of subballast has the influence of the order of approximately 25% to 33%, whereas remaining variables can impact up to 10%.

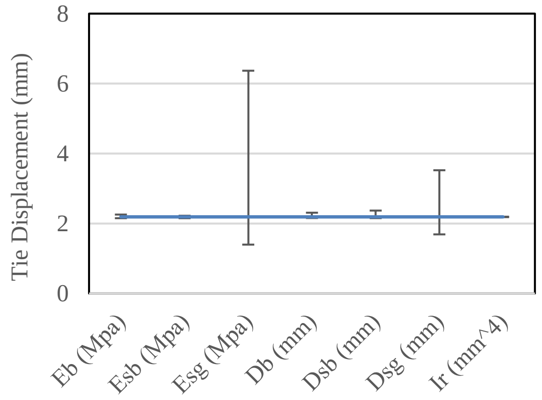


(a)

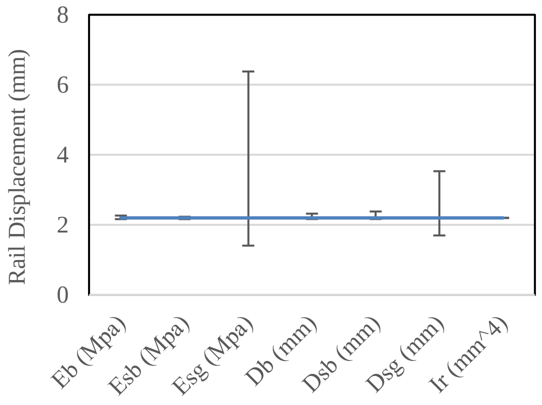


(b)

Figure 8 (a) Effects of selected parameters on rail vertical displacement and (b) on tie vertical displacement below the wheel load

Stress at the subgrade top is mostly affected by depth of subballast as seen in Figure 10(a). As the subballast depth decrease from 450 mm to 100 mm the stresses will increase by 127%. On the other hand, subgrade modulus, depth of ballast and depth subgrade caused 66%, 57% and 35% increases in the stresses respectively, when varied their values as described in Table 4.

The biggest impact on the track modulus, calculated using Equation 11 [Stewart and Selig (1982)], is observed due the subgrade modulus and then by depth of subgrade as shown in Figure 10(b).

$$u = \frac{1}{4}\sqrt[3]{\left[\frac{Q}{y_r}\right]^4 \frac{1}{E_r I_r}} \tag{11}$$

A reduction in subgrade modulus form 10 MPa to 60 MPa can lower the track modulus by 87%. Similarly, increasing subgrade thickness from 1500 mm to 3000 mm can lower the track modulus by around 62 %.

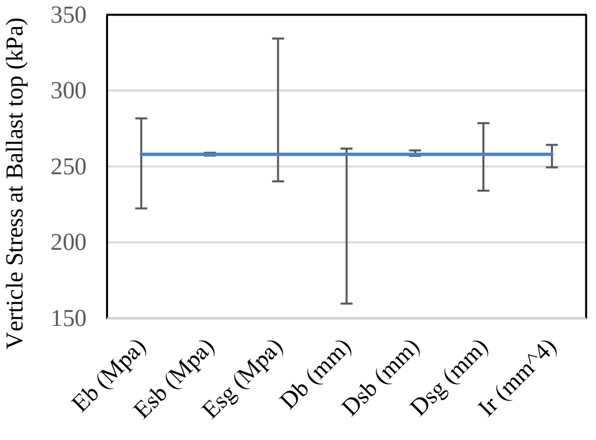


(a)

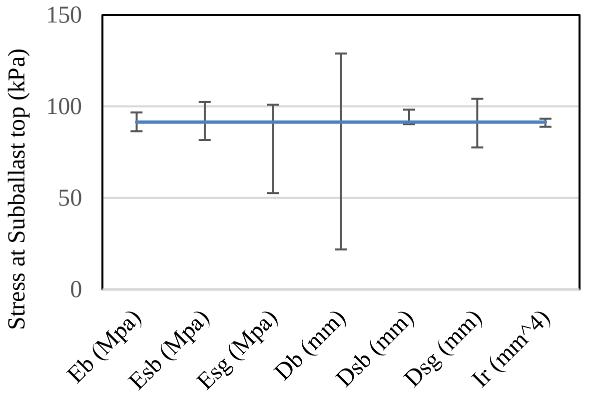


(b)

Figure 9 Effects of selected parameters on vertical stress at the top of (a) ballast layer and (b) subballast layer below the wheel load

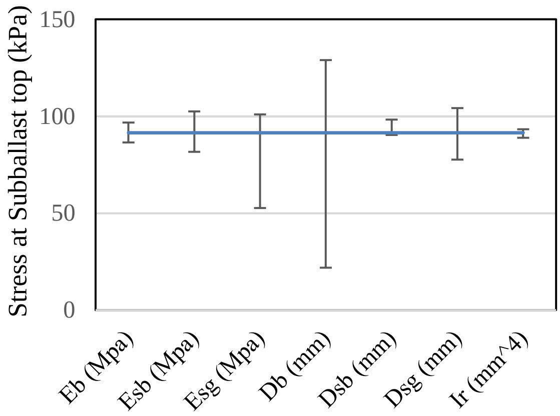


(a)

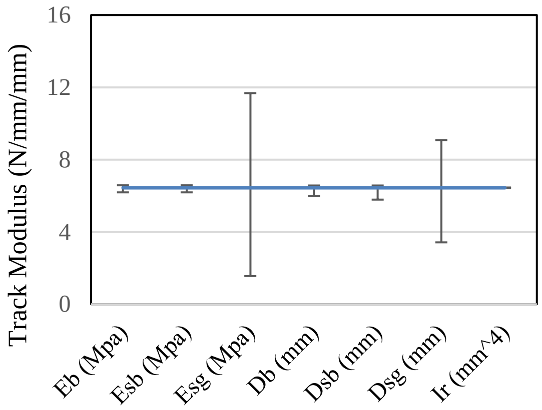


(b)

Figure 10 Effects of selected parameters on (a) vertical stress at the top of subgrade layer below the wheel load and (b) track modulus

Modulus of subgrade is found to be the most influential parameter to affect the common responses of the trackbed including rail and tie displacements; and stresses at the top of ballast, subballast and subgrade layers. The second most influential parameter is the depth of ballast which significantly affect the stresses at the top of substructure granular layers. However, it has negligible to little effect on the track modulus and rail and tie displacements. Thirdly, the depth of subgrade layer has moderate to considerable effect on all studied responses. Also, the modulus of ballast, subballast and subgrade has considerable effect on the stresses at the top of their respective layers. The least influential parameters were the rail moment of inertia and depth of subballast layer.

## 5. CONCLUSIONS

This paper introduces the development of the ADYTrack model. The initial results of building a capability are presented to analyse and design the railroad trackbeds more accurately and economically using more accurate subgrade information. The conclusions from this paper can be presented below:

1) A brief description of the model is provided with the details of the geometry, loading conditions, boundary conditions and quick review of mechanics involved with 8-nodal isoperimetric hexahedral brick elements.
2) The comparison with between the ADYTrack model and the other models available in the literature validated the predictions of vertical displacements and stresses along the depth below wheel load. The ADYTrack model predicted the vertical displacements along the depth below wheel load with almost less than 10% difference from PSA, MULTA and 3D20N models. Only the ILLITRACK predictions were off from all other model predictions by more than 100%. Furthermore, vertical stresses calculated by ADYTrack at the top of the subgrade are matching with PSA calculations with less than 5%, whereas the same is overestimating the stresses as compared to MULTA and 3D20N models by around 75% and is underestimating when compared with ILLITRACK calculations by almost 36%.
3) A detailed parametric study is conducted to study the effects of modulus and depths of ballast, subballast and subgrade, and the moment of inertia of rails. The studied responses are rail and tie displacements; stresses at the top of substructure layers and the track modulus. All the studied responses are most influenced by modulus of subgrade (of the order of 30-450 %) for the selected range of variation in the magnitude of independent variables. Similarly, the depth of ballast is observed the second most important parameter for stresses at the top of granular layers with its influence of the order of 40-500 % for the same variation in values. This study also finds that modulus of ballast and subballast layers has little effect on the stresses at the top of their respective layers (of the order of 15-20 %). The depth of subballast and rail moment of inertia are found the least influential parameters in this study (less than 10%).

## 6. ACKNOWLEDGEMENT

The authors would like to acknowledge and appreciate the Upper Great Plains Transportation Institute (UGPTI) at North Dakota State University for their financial and administrative support to conduct this study.

## 7. REFERENCES


Adegoke, C. W., Chang, C. S., and Selig, E. T. (1979) "Study of analytical models for track support systems." Transportation Research Record.733, Transportation Research Board, Washington, D.C., 12–20.

Barksdale, R. D. (1975). "Test procedures for characterizing dynamic stress-strain properties of pavement materials." Spec. Rep. 162, Transp, Res. Board, Washington, D.C.

Bathe, K.-J. and Wilson E. L. (1976) "Numerical Methods in Finite Element Analysis", Prentice-Hail

Burmister, D.M. (1945) "The general theory of stresses and displacements in layered systems — I, II and III". Journal of Applied Physics, 16: 88–302.

Chandrupatla T.R. and Belegundu A.D. (1997) "Introduction to Finite Elements in Engineering". Prentice Hall, New Jersey.

Chang I. C. (1975) "Track Foundation Stresses under Horizontal Loads". M. S. thesis, Department of Civil Engineering, Illinois Institute of Technology, Chicago.

Chang, S.C., Adegoke, C.W., and Selig, E.T. (1980) "Geotrack model for railroad track performance". Journal of the Geotechnical Engineering Division, ASCE, 106: 1201–1217.

Chen, W., Cheung, Y.K. (1992) "Three-dimensional 8-node and 20-node refined hybrid isoparametric elements". International Journal for Numerical Methods in Engineering, 35 (9), pp. 1871-1889.

Chu K. -H., Martin G. C., and Ma D. C. C. (1977) "Track Foundation Stresses under Vertical Loading". Rail International, pp. 617-626.

Clarke C. W. (1957) "Track Loading Fundamentals: 1". Railway Gazette, Vol. 106, No. 2, pp. 45-48.

Crawford J.E. (1972) "An Analytical Model for Airfield Pavement Analysis". Air Force Weapons Laboratory, Kirtland Air Force Base, NM, Rept. AFWLTR-71-70.

Feng Huang. (2011) "3D-models of Railway Track for Dynamic Analysis". MS thesis, KTH, Stockholm. RITA-VBT 11:16 ISSN 1650-867X ISRN KTH/VBT-11/16-SE.

Herrman L. R. (1968) "User's Manual for PSA: Three-Dimensional Elasticity Analysis of Periodically Loaded Prismatic Solids". Univ. of California, Davis.

Hetenyi M. (1946) "Beams on Elastic Foundations". Univ. of Michigan Press, Ann Arbor.

Huang, Y. H., Lin, C., Deng, X., and Rose, J., (1984) "KENTRACK, A Computer Program for Hot-Mix Asphalt and Conventional Ballast Railway Trackbeds", Asphalt Institute (Publication RR-84-1) and National Asphalt Pavement Association (Publication QIP-105), 164 pages.

Jog C.S. (2005) "A 27-node hybrid brick and a 21-node hybrid wedge element for structural analysis". Finite Elem Analysis Design, 41, pp. 1209–1232.

KENTRACK Version 2.0.1, (2006) Program, Help File and Example Data Files, Department of Civil Engineering, University of Kentucky.

Li D., Hyslip J.P., Sussmann T.R., Chrismer S.M. (2015) "Railway Geotechnics". CRC Press/Taylor & Francis Group, Boca Raton, FL, USA

Liu, S. (2013) "KENTRACK 4.0: A Railway Trackbed Structural Design Program." MSc Thesis, University of Kentucky.

MacNeal R.H., Harder R.L. (1985) "A proposed standard set of problems to test finite element accuracy". Finite Elem Analysis Design, 1, pp. 3-20.

Meacham H. C. et. al. (1968) "Study of New Track Structure Design". Battelle Memorial Institute, Columbus, OH; U.S. Department of Transportation, Summary Report.

Mishra D., Sharma S., Shrestha A., Li D. and Basye C. (2016) "GEOTRACK-2015: An upgraded software tool for railroad track analysis". Proceedings of the ASME Joint Rail Conference 2016.

Monismith C. L. and Finn F. N. (1975) "Flexible Pavement Design: State-of-the-Art-1975". Transportation Engineering Journal, Proc., ASCE, Vol. 103, No. TE 1, pp. 1-53.

Pichumani R. (1973) "Finite Element Analysis of Pavement Structures Using AFPAV Code (Linear Elastic Analysis)". Air Force Weapons Laboratory, Kirtland Air Force Base, NM, Rept. AFWL-TR72-186, May 1973. NTIS: PB 239/244/7SL

Robnett Q. L., Thompson M. R., Knutson R. M., and Tayabji S. D. (1976) "Development of a Structural Model and Materials Evaluation Procedures". Federal Railroad Administration, Rept. FRA/ORD-76-255, NTIS: PB 262 987/lSL.

Rose, J. G., Agarwal, N. K., Brown, J. D., and Ilavala, N. (2010) "KENTRACK, A Performance-Based Layered Elastic Railway Trackbed Structural Design and Analysis Procedure– A Tutorial." In Proceedings of the 2010 Joint Rail Conference, 73-110.

Rose, J., Liu, S., and Souleyrette, R. R. (2014) "Kentrack 4.0: A Railway Trackbed Structural Design Program." In Proceedings of 2014 Joint Rail Conference.

Rose, J.G., Brown, E.R. and Osborne, M.L., (2000) "Asphalt Trackbed Technology Development – The First 20 Years". Transportation Research Record 1713, Transportation Research Board, pp.1-9

Selig, E. T., and Waters, J. M. (1994) "Track geotechnology and substructure management". Thomas Telford Services Ltd., London, U.K.

Selig, E.T., Chang, C.S., Adegoke, C.W., and Alva-Hurtado, J.E. (1979) "A theory for track maintenance and life prediction". Department of Civil Engineering, State University of New York at Buffalo, Report DOT/RSPA/DPB-50/79/22.

Selvadurai, A. P. S. (1979), "Elastic Analyses of Soil-Foundation Interaction". Elsevier Scientific Publishing Co

Shahu, J. T., Rao, N. S. V. K., and Yudhbir, (1999) "Parametric study of resilient response of tracks with a sub-ballast layer." Can. Geotech. J., 36(6), 1137–1150.

Stewart H.E. (1988) "User's Manual for GEOTRACK Computer Program (VAX Version)".

Stewart, H.E., and Selig, E.T. (1982) "Predicted and measured resilient response of track". Journal of the Geotechnical Engineering Division, ASCE, 108: 1423–1442.

Strang, G. and G. J. Fix. (1973) "An Analysis of the Finite Element Method". Englewood Cliffs: Prentice–Hall, Inc.

Sze KY, Fan H. (1996) "An economical assumed stress brick element and its implementation". Finite Elem Analysis Design, 21, pp.179–200.

Talbot, A.N. (1933) "Stresses in railroad track". Sixth Progress Report of the Special Committee on Stresses in Railroad Track. In Proceedings of AREA (Bulletins) American Railway Engineering Association (AREA). Vol. 45. pp. 68–848.

Tayabji S. D. and Thompson M. R. (1976a) "Program ILLI-TRACK: A Finite-Element Analysis of Railway Track Support System-User's Manual". Federal Railroad Administration, Rept. FRA/ORD-76-257.

Tayabji S. D. and Thompson M. R. (1976b) "Track Support System Parameter Study". Federal Railroad Administration, Rept. FRA/ORD-76-256. NTIS: PB 263-370/9SL.

Winkler, E. (1865) Die Lehre von der Elastizist und Festiekeit (Praga Dominicus, 1:367), p. 182.

Zienkiewicz, O. C. and Cheung Y. K. (1965) "Finite Elements in the Solution of Field Problems". The Engineer, pp. 507-510.

Zienkiewicz, O. C. (1977) "The Finite Element Method", 3rd ed., McGraw-Hill, London